Sponges against miR-19 and miR-155 reactivate the p53-Socs1 axis in hematopoietic cancers

Lian Mignacca, Emmanuelle Saint-Germain, Alexandre Benoit, Véronique Bourdeau, Alejandro Moro, Gerardo Ferbeyre *

Département de biochimie et médecine moléculaire, Université de Montréal, C.P. 6128, Succ. Centre-Ville, Montréal, Québec H3C 3J7, Canada

ABSTRACT

Normal cell proliferation is controlled by a balance between signals that promote or halt cell proliferation. Micro RNAs are emerging as key elements in providing fine signal balance in different physiological situations. Here we report that STAT5 signaling induces the miRNAs miR-19 and miR-155, which potentially antagonize the tumor suppressor axis composed by the STAT5 target gene SOCS1 (suppressor of cytokine signaling-1) and its downstream effector p53. MiRNA sponges against miR-19 or miR-155 inhibit the functions of these miRNAs and potentiate the induction of SOCS1 and p53 in mouse leukemia cells and in human myeloma cells. Adding a catalytic RNA motif of the hammerhead type within miRNA sponges against miR-155 leads to decreased miR-155 levels and increased their ability of inhibiting cell growth and cell migration in myeloma cells. The results indicate that antagonizing miRNA activity can reactivate tumor suppressor pathways downstream cytokine stimulation in tumor cells.

© 2016 Elsevier Ltd. All rights reserved.

1. Introduction

Cytokine signaling converges into the activation of key transcription factors which control the expression of genes allowing for the expansion of certain lineages of hematopoietic cells [1]. Many genes codings for transcription factors and cytokine signaling proteins are mutated or overexpressed in hematopoietic cancers. Another layer of gene regulation altered in these cancers involves small regulatory RNAs known as miRNAs [2,3]. MiRNAs control gene expression at the post-transcriptional level [2], so their effects can further modify the gene expression pattern initially laid down by transcription factors.

One key transcription factor whose activity is deregulated in multiple hematopoietic cancers is STAT5 [1]. In normal cells, STAT5 activation does not cause neoplastic transformation. Tumor suppressor genes activated by STAT5 signaling avoid uncontrolled cell proliferation and neoplastic transformation. STAT5 can induce the expression of the suppressor of cytokine signaling SOCS1, which can exert tumor suppression by two mechanisms. First, SOCS1 controls JAK kinases signaling downstream of cytokine receptors preventing constitutive cytokine stimulation [4]. Second, SOCS1

can bind p53 facilitating its activation by DNA damage signaling [5–8]. However, SOCS1 expression is often silenced in hematopoietic cancers by DNA methylation [9–12]. In addition, miRNA mediated repression is emerging as an important mechanism to prevent SOCS1 expression in cancer [7,13–17]. One important question is whether it is possible to restore SOCS1 expression and its ability to engage the p53 tumor suppressor pathway by targeting miRNAs in hematopoietic cancers. Here we show that targeting miR-155 or miR-19 in mouse and human hematopoietic cancer cell lines increases SOCS1 levels, leading to enhanced p53 activity and inhibition of the transformed phenotype.

2. Experimental procedures

2.1. Cell lines and reagents

Raw264.7 (ATCC TIB-71) a murine leukemia cell line transformed with the Abelson leukemia virus and IMR90 (ATCC CCL-186) were purchased from American Type Culture Collection (ATCC) and cultured in DMEM (GIBCO, Burlington, ON, Ca). RPMI8226 (ATCC CCL-155) was purchased from ATCC and cultured in RPMI-1640 (GIBCO). Both media were supplemented with 10% fetal bovine serum (FBS, Hyclone, Logan, UT, USA) and 1% penicillin G/streptomycin sulfate (Wisent, St-Bruno, Qc, Canada). LPS (TLR4 ligand) from *Escherichia coli* strain 055:B5 re-extracted by phenol chloroform (Sigma–Aldrich, St Louis, MO, USA) was used at a

* Corresponding author at: Université de Montréal, Département de biochimie et médecine moléculaire, E-515, C.P. 6128, Succ. Centre-Ville, Montréal, Québec H3C 3J7, Canada.

E-mail address: g.ferbeyre@umontreal.ca (G. Ferbeyre).

concentration of 500 ng/ml. Doxorubicin (Sigma) was used at a concentration of 1 μM.

2.2. Plasmid constructions

Ca-STAT5A was described in [18]. Multimerized microRNA binding sites (RNA sponges) in the retroviral vector pPIG were kindly provided by Kluiver et al. [19]. Two constructs target miR-19 and contain either 6 miRNA binding sites (MBS) or 20 MBS. One construct targets miR-155 and contains 14 MBS. For the catalytic sponge, the hammerhead ribozyme sequence was embedded within the MBS (Table SI). Synthetic double stranded oligonucleotides (GeneArt, ThermoFischer Sc.) containing two copies of the catalytic sponge sequence (Supplemental Table I) were digested with SanD1 and cloned into pPIG according to Kluiver et al. [19]. We made two catalytic constructs against miR-155, one containing 14 MBS and the other 18 MBS. For the luciferase reporter, four binding sites for either miR-19 or miR-155 were cloned in the 3'UTR of the firefly luciferase gene encoded in the pmirGLO reporter system. Binding sites were replaced by their reverse-complement as a control. The shRNA against p53 was from [20].

2.3. Retroviral infection of cells

Retroviral-mediated gene transfer was performed as previously described [21]. For RPMI8226, 293T cells were transfected with 15 μg vector DNA and 15 μg of packaging vector pCL10A1 (a kind gift of Dr. Moshe Talpaz). Media of 293T cells were changed 24 h post-transfection. Half the viral soup was then added to 2×10^6 cells in a 6 well-plate. Spin-infections were performed by centrifugation of the cells at 3200 rpm with the viral soup for three hours at 32 °C. An equal volume of fresh medium was then added to the cells for an overnight incubation. The next day, medium of the infected cells was changed and selections started 6–8 h later. Infected cell populations were selected with either puromycin (2.5 μg/ml, 3 days) or hygromycin (100 μg/ml, 5 days).

2.4. Preparation of cell extracts and analysis by Western blotting

Cells were washed twice using PBS, harvested in 500 μl of RIPA buffer (150 mM NaCl, 1% NP-40, 0.5% deoxycholate, 0.1% SDS, 50 mM Tris–HCl, pH 8, and 5 mM EDTA), incubated on ice for 5 min and sonicated for 10 s. Protein samples were prepared in 4X Laemmli buffer and heated at 95 °C for 5 min. SDS–PAGE and western blotting were performed as described previously [22]. Proteins were loaded on a 10% SDS–PAGE and transferred to Immobilon-P membranes (Millipore, Billerica, MA, USA). The primary antibodies used were as follows: anti-phospho-Stat5[Y694] (#9314; 1:1000; Cell signaling, Danvers, MA, USA), anti-Stat5 (#9363; 1:1000; Cell signaling), anti-Socs1 (4H1; 1:1000; MBL, Moburn, MA, USA), anti-phospho-p53[S15] (#9284; 1:1000; Cell signaling), anti-p21 (clone C-19; SC-397; 1:750; Santa Cruz, Dallas, Texas, USA), anti-p53 (clone DO-1; SC-126; 1:1000; Santa Cruz) and anti-tubulin (B-512; 1:20000; Sigma–Aldrich). Signals were revealed with secondary antibodies coupled to peroxidase (BioRad, Mississauga, ON, Canada) by using ECL or ECL prime (GE healthcare, Baie d'Urfé, Qc, Canada).

2.5. Luciferase assays

Twenty-four hours before transfection, Raw264.7 were seeded at 200000 cells per well in a 12-wells plate. The pmirGLO vector (100 ng) was transfected using X-treme GENE HP (Sigma) with a transfection reagent-reporter ratio of 2:1. The medium was changed after 24 h. For experiments that required LPS treatment, the latter was added to fresh medium and cells were incubated for a further four hours. Luciferase activity was assayed using the Dual-Luciferase Reporter Assay System (Promega, Madison, WI, USA).

2.6. Real-time quantitative PCR

Total RNA was isolated using Trizol (Invitrogen). Reverse transcription and real-time PCR was performed as previously described [23]. The mRNA expressions were measured relative to those of β-actin and TBP mRNA. For miRNA detection, a polyA tail was added to 2 μg of total RNA extract using 2.5 U of *E.coli* PolyA polymerase (NEB). Tailed total RNA was reverse transcribed using an anchor primer as described by Luo et al. [24]. cDNA was generated using the RevertAid H Minus First Strand cDNA Synthesis Kit (Fermentas, Thermo Fisher Scientific, MA, USA). The qPCR reaction was carried in a final volume of 10 μl and contained 1 μl reverse transcription products diluted 120-fold, 10 μM forward primer, 10 μM universal reverse PCR primer, 1 μl 10X PCR buffer, 200 μM of each dNTP, 0.5 U of JumpStart Taq DNA polymerase, and 0.05 μM of universal TaqMan probe. The mixture was incubated as described by Luo et al. [24]. Data were normalized using endogenous controls miR-191 and U6. All forward and reverse primers are listed in Supplementary Table 1 (S1).

2.7. Growth curves and Methylcellulose assay

Either empty MSCVhygro- or ca-STAT5A-expressing Raw264.7 cells were seeded at a concentration of 2500 cells/ml and grown in six well-plates in triplicate for one week. Cells were washed with PBS and fixed with a 1% glutaraldehyde solution in PBS. Cells were then stained with 0.5% crystal violet and rinsed several times with water before being left to dry. Retained dye was extracted with two ml of 10% acetic acid and 200 μl of extracted dye was used for absorbance measurements at 590 nm using a 96-well plate and a microplate reader. RPMI8226 cells were seeded at a concentration of 5000 cells/mL and grown in cell culture flasks in triplicate for one week. Cells were regularly counted with a cell counter.

Colony formation capacity was measured for RPMI8226 by performing a methylcellulose assay. RPMI8226 cells were stably transduced by retroviral infection with empty vector, normal sponge against miR-155 or catalytic sponges against miR-155. 4000 cells were diluted into 250 μL of methylcellulose solution (R&D Systems Inc. catalogue #HSC001), final concentration 1.27% in RPMI1640 medium supplemented with 20% FBS. Cells were then plated in 24-well plates, in triplicates, and grown in semi-solid medium for two weeks at 37 °C with 5% CO_2. Colonies with more than 50 cells were counted under a light microscope.

2.8. Migration assay

Cell migration was measured *in vitro* by using Transwell chambers (8 μm pore size, Corning #C3422) inserted in a 24-well plate and 3×10^5 stably infected cells were then plated in the top chamber in 100 μL of RPMI1640 medium supplemented with 10% FBS. In the bottom chamber, we placed 600 μL of RPMI1640 medium supplemented with 20% FBS. Cells were incubated for 24 h and the cells in the bottom compartment (migrated cells) were counted. Every condition was done in triplicate.

3. Results

3.1. A constitutively active form of STAT5A induces miR-19 and miR-155

To characterize how STAT5 activity regulates the expression of SOCS1 and miRNAs that target SOCS1, we introduced a constitutively active allele of STAT5A (caSTAT5A) in normal human fibroblasts IMR90. In these cells, caSTAT5A induces an antiproliferative response known as cellular senescence [5] characterized by a reduction in the proliferation marker KI67 (Fig. 1A). CaSTAT5A also induces high levels of SOCS1 (Fig. 1B) which we showed previously required for p53 activation and senescence [5]. caSTAT5A induces the expression of miRNAs of the cluster miR17-92 (including miR-19) (Fig. 1C), and miR-155 (Fig. 1D). We also expressed caSTAT5A in the murine leukemia cell line Raw264.7 and observed no increase in already well-expressed mature miR-19 (Fig. 1E) but a significant induction of miR-155 (Fig. 1F). Both miR-19 [16] and miR-155 target SOCS1 [7,14,15]. As shown for normal human fibroblasts, expression of caSTAT5A in Raw264.7 cells induced a growth arrest (Fig 1G). In Raw264.7 cells expressing caSTAT5A, both miR-19 and miR-155 were more active as measured using miRNA reporters containing binding sites for miR-19 or miR-155 in the 3'UTR of a luciferase mRNA (Fig 1H and I).

3.2. MiRNA sponges can inhibit miR-19 and miR-155 activity in Raw264.7 cells

The action of miRNAs can be inhibited by RNA sponges, which are multimerized miRNA binding sites. Sponges can be expressed in cells to titrate any desired miRNA. Kluiver and colleagues generated miRNA sponges against miR-19 and miR-155 [19]. To investigate the functional importance of the SOCS1-p53 axis in a system that engages endogenous molecules, we treated Raw264.7 cells expressing these sponges with LPS, which is known to induce Stat5 in these cells [25]. The use of LPS thus helps to capture the dynamics of miRNA induction and activity shortly after perturbing the cells.

We treated Raw264.7 cells with a combination of LPS and doxorubicin to simultaneously study the interactions between Socs1 (induced by LPS) and p53 (induced by doxorubicin). We first investigated whether treatment of Raw264.7 with LPS could induce miR-19 and miR-155. We expected this because there are Stat5 binding sites in the promoters of miR-155 [26] and the cluster of miRNAs miR-17-92 that contains miR-19 [27]. We first confirmed that treatment of Raw 264.7 cells with LPS induced phosphorylation of endogenous Stat5A (Fig. 2A). We also found that LPS induced miR-19a (Fig. 2B) and miR-155 (Fig. 2C) in Raw264.7 cells although with different kinetics. The miR-19 family of miRNAs was induced at four hours after treatment and remained elevated for
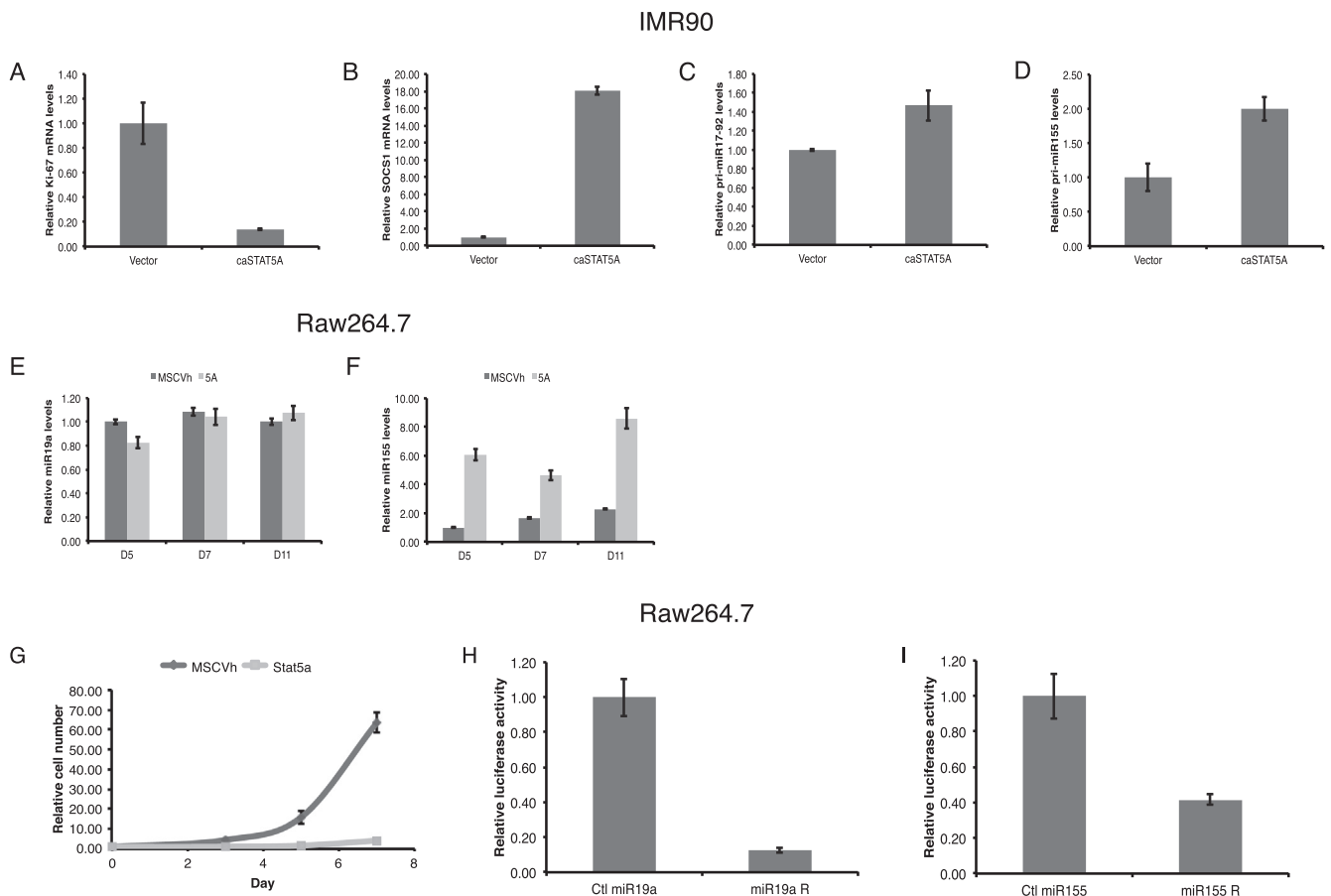
Fig. 1. A constitutively active form of STAT5A induces miR-19 and miR-155. QPCR for (A) KI-67, (B) SOCS1, (C) primary miR17-92 and (D) primary miR-155 of IMR90 expressing either an empty vector control or ca-STAT5A. (E and F) qPCR for miR-19a (E) and miR-155 (F) of Raw264.7 expressing either an empty vector control (MSCVh) or ca-STAT5A at 5, 7 or 11 days post-infection. (G) Growth curves of Raw264.7 cells infected with an empty control vector or ca-STAT5A. Data are presented as mean ± SD of triplicates. (H and I) Luciferase activity from Raw264.7 cells stably expressing ca-STAT5A and transfected with miR-19 or miR-155 luciferase reporters (R).
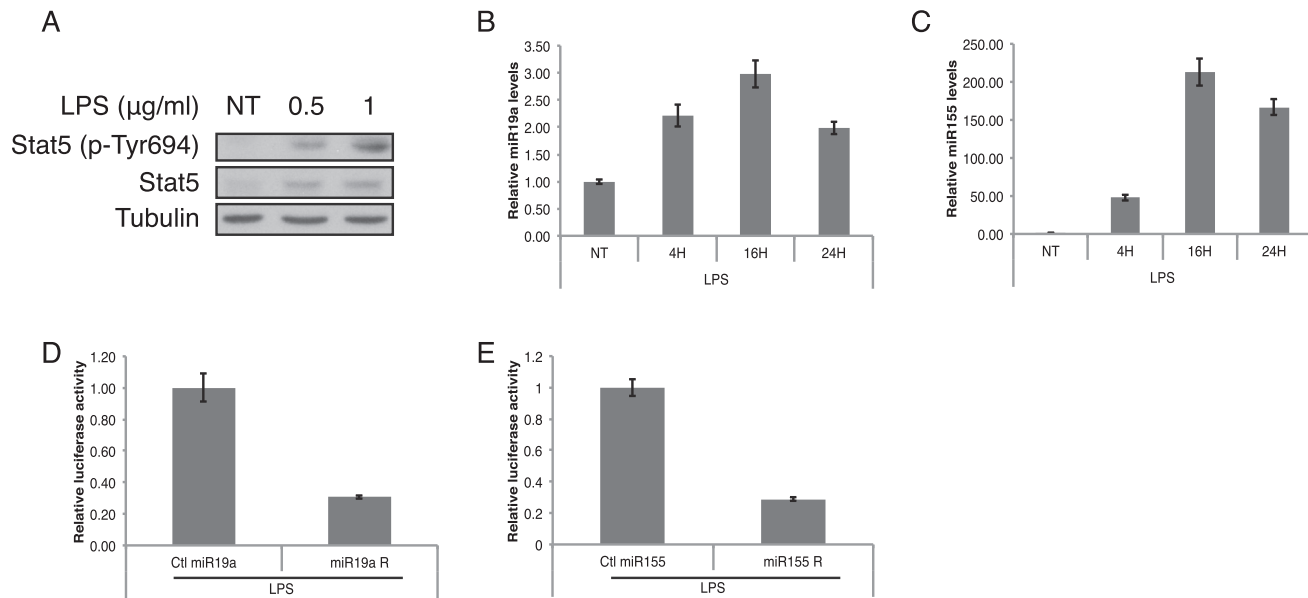
Fig. 2. LPS treatment induces Stat5a, miR-19 and miR-155 in Raw264.7 cells. (A) Immunoblots for phosphorylated Stat5 (Tyr694) and total Stat5 using cell lysates from Raw264.7 cells stimulated with LPS. (B-C) qPCR for miR-19a and miR-155 induced in Raw264.7 cells by LPS. (D and E) Luciferase activity from LPS treated Raw264.7 cells transfected with miR-19 or miR-155 luciferase reporters®.

24 h. The induction of miR-155 also started at 4 h after treatment and remained elevated for 24 h but it was more substantial than that of miR-19, reaching 200 fold. Expression of miRNA reporters containing binding sites for miR-19 or miR-155 in the 3'UTR of a luciferase gene revealed that these miRNAs are active in Raw 264.7 cells treated with LPS (Fig. 2D and E).

Since SOCS1 is among miR-19 and mir-155 targets [7,14,15], we reasoned that inhibiting their functions should lead to higher Socs1 levels in Raw 264.7 cells treated with LPS. We thus expressed anti-miR-19 and anti-miR-155 sponges in Raw 264.7 cells treated with LPS to induce Stat5 and Socs1 and doxorubicin to activate p53. The

presence of miRNA sponges increased the induction of Socs1 protein levels by LPS (Fig. 3A). We reported a few years ago that Socs1 facilitates phosphorylation of p53 at serine 15 by binding both p53 and activated ATM/ATR as part of DNA damage signaling [5]. As expected from this mechanism, LPS and doxorubicin treatments stimulate phosphorylation of p53 at serine 15. However, miRNA sponges enabled an increase in time and intensity of the phosphorylation of p53 at serine 15 (Fig. 3B). It is known that the dynamics of p53 induction affect target gene expression, suggesting that miRNAs can modulate the p53 response via this mechanism [28]. Consistent with this explanation, sponges against miR-155 indeed
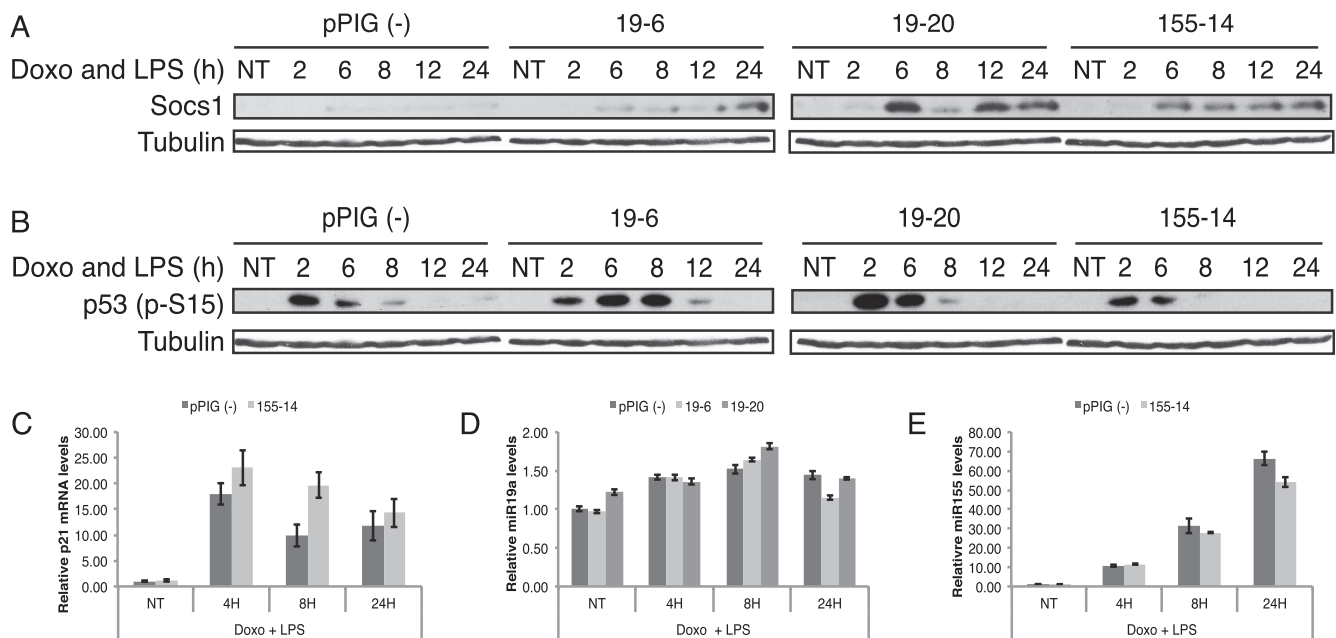
Fig. 3. MicroRNA sponges against miR-19 or miR-155 stabilize Socs1 protein and increase p53 phosphorylation and activity in response to doxorubicin and LPS. (A) Immunoblots for Socs1 using cell lysates from Raw264.7 cells stably expressing an anti-miR-19 sponge or an anti-miR-155 sponge and stimulated with doxorubicin (doxo) and LPS. pPIG is the control vector. (B) Immunoblots for phosphorylated p53 (Ser15) using cell lysates as in A. (C) QPCR for p21 using cell extracts as in A. (D) QPCR for miR-19a of Raw264.7 stably expressing anti-miR-19 sponges and stimulated with doxo and LPS. (E) QPCR for miR-155 of Raw264.7 stably expressing an anti-miR-155 sponge and stimulated with doxo and LPS.

increased the expression of the p53 target gene p21 (Fig. 3C). We also measured the effect of the sponges on the levels of miR-19 and miR-155. We did not find any reduction in miRNA levels in cells expressing miRNA sponges (Fig. 3D and E), suggesting that they act by competitively titrating miRNAs out of their targets.

3.3. The next generation of miRNA sponges

We next tested a novel sponge formulation where a catalytic RNA motif of the hammerhead type was added to the RNA sponge. It is expected that the hammerhead ribozyme will cleave the mature miRNA (Fig. 4A). We performed this study in a human myeloma cell line, which is more relevant for human cancer and expresses high levels of miR-155. Expression of sponges with 14 binding sites for miR-155 in the human myeloma cell line RPMI8226 reduced the levels of miR-155 and this reduction was more pronounced when a hammerhead catalytic RNA motif was included in each miRNA binding site in sponges with either 14 or 18 binding sites (Fig. 4B, left). We also measured the level of the non-guide (passenger) strand of the miR-155 precursor and observe only a moderate reduction by the catalytic sponges with 18 miR-155 binding sites (Fig. 4B, right). The catalytic sponges were also the most effective in reducing cell growth in these cells (Fig. 4C). In a long-term proliferation assay on cells plated on

methylcellulose, sponges reduced colony formation and again the catalytic sponges were more effective (Fig. 4D and E). We also tested sponges on the ability of RPMI8226 to migrate in a transwell assay. Once again catalytic sponges reduced cell migration in comparison with the control vectors or the non-catalytic sponge, which had an intermediate effect (Fig. 4F). Catalytic sponges were very effective in inducing levels of SOCS1 mRNA, consistent with their ability to inhibit miR-155 (Fig. 4G). The levels of RNAs coding for the sponges were reduced in comparison with the control sponge likely because cells with the highest levels of sponges are counter selected. It is also possible that endogenous miRNAs can decrease sponge levels in the same way they can reduce mRNA target levels [29].

Next, we studied whether inhibition of miR-155 in RPMI8226 engaged the p53 pathway as in Raw264.7 cells. Catalytic sponges increased the levels of phosphorylated p53 at serine 15 and the p53 target p21 better than non-catalytic sponges in RPMI8226 (Fig. 5A). P53 targets NOXA, GADD45B and ABHD4 were also moderately induced while the p53-repressed gene BCAT1 was also slightly reduced (Fig. 5B). More importantly, p53 knockdown by a validated shRNA restored the ability of these cells to form colonies when plated on methylcellulose (Fig. 5D) indicating that the growth defect of cells expressing anti-miR-155 sponges was p53 dependent. However, the migration capacity of the p53-depleted
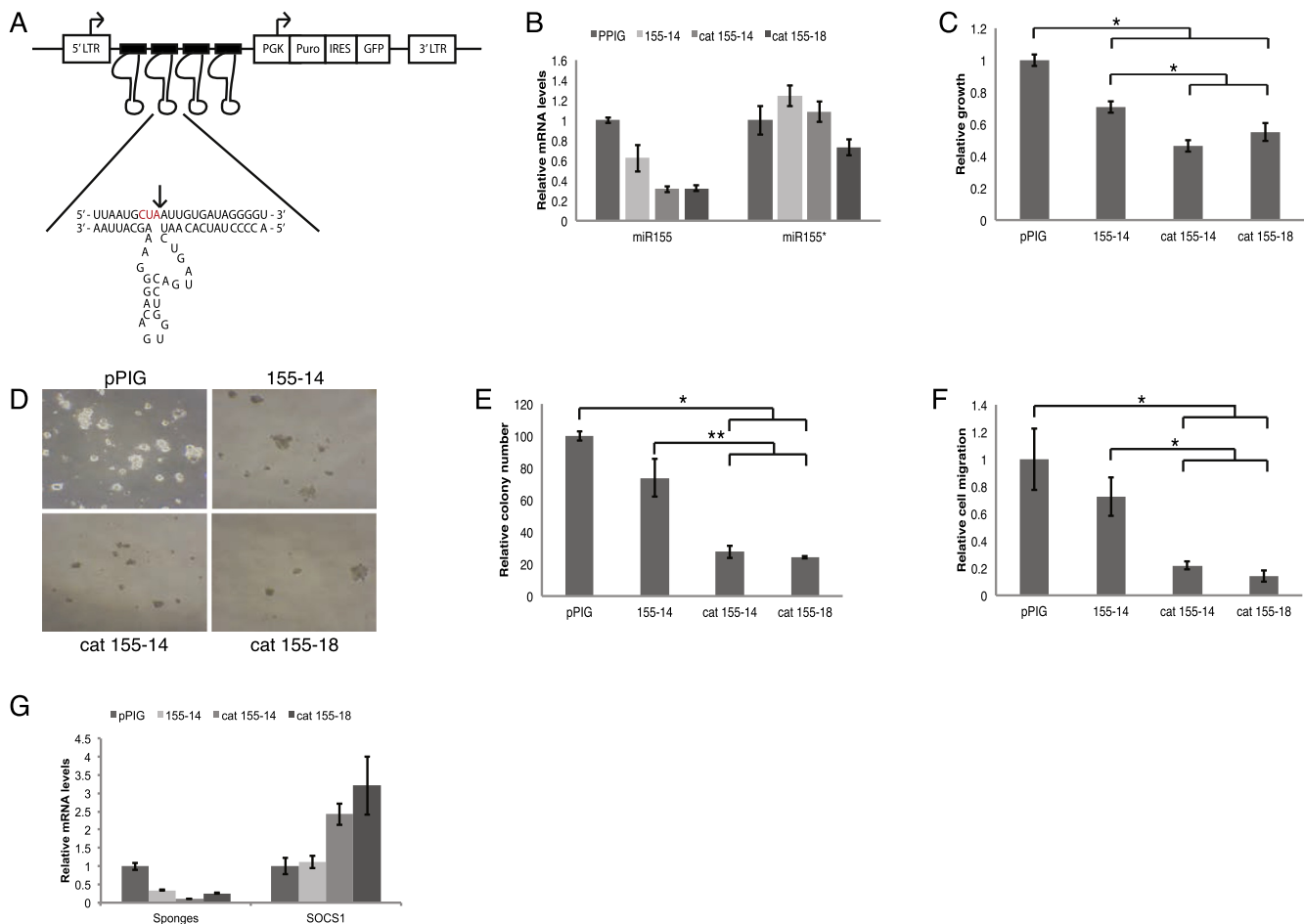
Fig. 4. Catalytic sponges against miR-155 inhibit the transformed phenotype of human myeloma cells. (A) Retroviral vector expressing a catalytic sponge. The hammerhead ribozyme motif and the cleavage site on the target are indicated. Hammerhead ribozymes cleave the target after the consensus sequence *NUX*, where *X* is everything but a G. (B) QPCR for miR155 (mature, guide strand) or miR155* (passenger strand) of RPMI8226 stably expressing an anti-miR-155 sponge or its catalytic version. pPIG is the control vector. (C) Growth assay performed on RPMI8226 cells stably expressing normal or catalytic sponges against miR-155. The number of colonies was quantified one week after seeding. (D and E) Methylcellulose colony formation assays were performed using the same cells as described in C. (F) Migration assay performed with the same cells as in (C) using Transwell plates (see Section 2). Migration counts were done 24 h after plating. (G) QPCR for the sponges and SOCS1 using the same cell extracts as in (B).
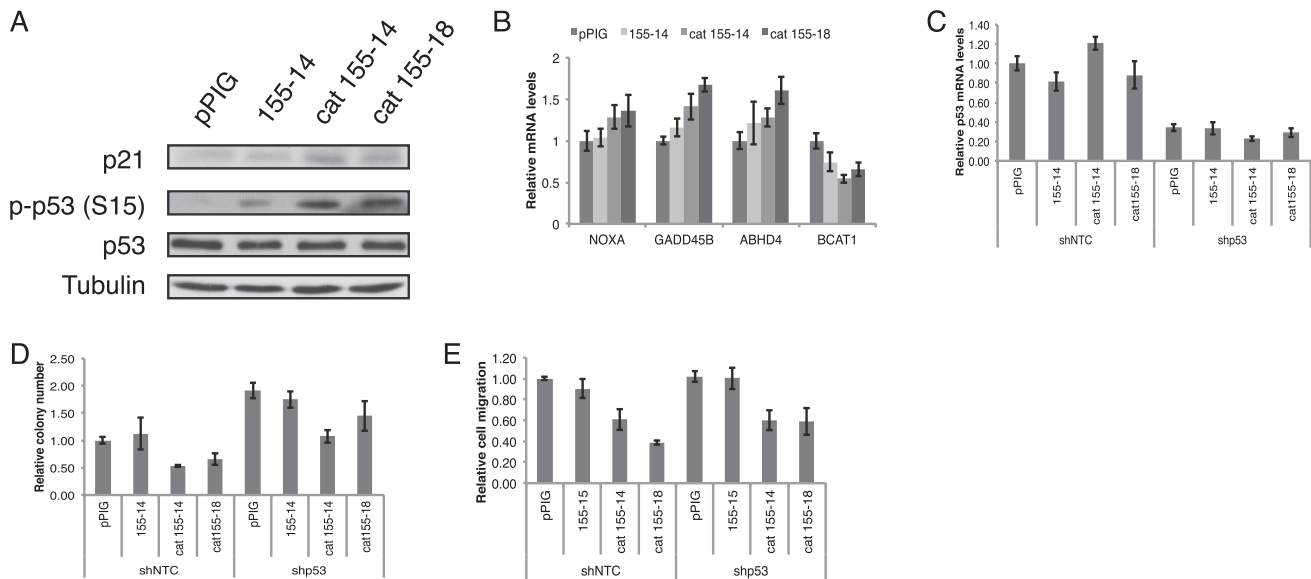
Fig. 5. The catalytic sponge effect is dependent on the p53 pathway. (A) Immunoblots of RPMI8226 cells expressing the regular sponge or the catalytic sponges. (B) QPCR for p53 targets in RPMI8226 using the same cell extracts as in A. (C) QPCR for p53 in RPMI8826 cells stably expressing the regular sponge or its catalytic version in combination with an shRNA against p53 or a control shRNA (shNTC). (D) Methylcellulose colony formation assay performed with the same cells as described in D. (E) Migration assay of RPMI8226 stably expressing the indicated sponges in combination with an shRNA against p53 or a shRNA control.

cells that expressed the sponges was not enhanced suggesting that miR-155 controls cell migration by another pathway (Fig 5E).

4. Discussion

The treatment of hematopoietic malignancies is mostly based on cytotoxic chemotherapy, which can be effective in some patients but is limited by toxicity and the development of resistance. Recently, novel therapies targeting specific genetic alterations in cancer cells have been introduced exemplified by the highly successful use of BCR-ABL inhibitors in chronic myelogenous leukemia [30]. It is hoped that identifying additional therapeutic targets in cancer cells can lead to equally effective treatments. MiRNAs have been proposed as therapeutic targets in cancer [31]. Several transcription factors with deregulated activity in hematopoietic cancers drive the expression of miRNAs [32]. Here we report that the miRNAs miR-19 and miR-155 control the outcome of STAT5 stimulation. High levels of these miRNAs modulate the activation of the SOCS1-p53 axis acting downstream of STAT5 to limit tumorigenesis [5,7]. The effects of miRNAs seem to affect the fine dynamics of p53 induction and phosphorylation, which is emerging as an important factor in the control of the p53 response [28]. These dynamics are difficult to study in non-synchronized cell cultures but the use of LPS and doxorubicin might have allowed us to capture it in a cell population.

To inhibit miRNAs, we used miRNA sponges of two kinds. First we used "traditional" sponges where the miRNA binding sites were multimerized and which act by titrating miRNAs. Second, we improved this formulation by adding catalytic RNA motifs of the hammerhead type within the miRNA binding site, which can potentially promote miRNA turnover and reduce miRNA levels. Although further studies are required to optimize catalytic RNA sponges, we were able to show that they reduce the steady state levels of mature miRNA targets in comparison with conventional sponges.

Inhibition of miR-19 and miR-155 activity can reactivate the expression of tumor suppressor genes such as SOCS1 and subsequently p53, which can then inhibit cell proliferation, cell migration and block tumor progression. However, we acknowledge

that in addition to Socs1, other targets of miR-19 and miR-155 are expected to be upregulated by sponges against these miRNAs and they could contribute to the phenotypic effects observed. However, since the kinetic of induction of these two miRNAs is not the same after treatment with LPS, it suggests that their simultaneous inhibition should bring a higher effect on their common targets. The identification of oncogenic miRNAs as potential targets to restore tumor suppression functions in cancer cells shows potential for cancer therapy. One interesting aspect of miRNAs functions in cancer is that they change the normal balance between signals that stimulate or antagonize cell growth (Fig. 6). Therefore inhibition of miRNAs can restore a normal physiological balance with little toxicity to normal cells. The possibility of translating our findings to the clinics is encouraged by clinical studies with locked nucleic
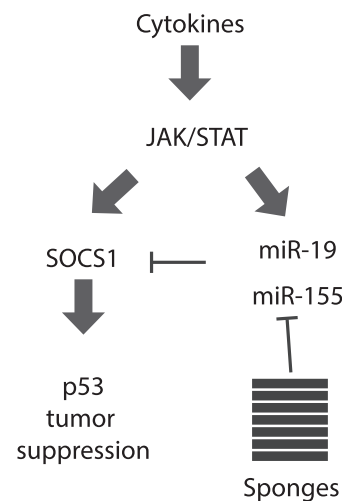
Fig. 6. MiRNA sponges restore normal balance between growth inhibitory and growth promoting pathways. Cytokine signaling induces both growth inhibitors (i.e. SOCS1) and miRNAs that modulate their expression (miR-19 and miR-155). These miRNAs are overexpressed in cancer cells but their inhibition with sponges restores a normal physiological equilibrium.

acids [33] which could be used to target miR-19 and miR-155 in hematopoietic cancers.

Conflict of interest

The authors declare that they have no conflict of interest.

Acknowledgments

Appendix A. Supplementary material

Supplementary data associated with this article can be found, in the online version, at http://dx.doi.org/10.1016/j.cyto.2016.01.015.

References

[1] G. Ferbeyre, R. Moriggl, The role of Stat5 transcription factors as tumor suppressors or oncogenes, Biochim. Biophys. Acta. 1815 (2011) 104–114.

[2] G. Marcucci, K. Mrozek, M.D. Radmacher, R. Garzon, C.D. Bloomfield, The prognostic and functional role of microRNAs in acute myeloid leukemia, Blood (2010).

[3] J. Chen, O. Odenike, J.D. Rowley, Leukaemogenesis: more than mutant genes, Nat. Rev. Cancer. 10 (2010) 23–36.

[4] S. Ilangumaran, R. Rottapel, Regulation of cytokine receptor signaling by SOCS1, Immunol. Rev. 192 (2003) 196–211.

[5] V. Calabrese, F.A. Mallette, X. Deschenes-Simard, S. Ramanathan, J. Gagnon, A. Moores, et al., SOCS1 links cytokine signaling to p53 and senescence, Mol. Cell. 36 (2009) 754–767.

[6] F.A. Mallette, V. Calabrese, S. Ilangumaran, G. Ferbeyre, SOCS1, a novel interaction partner of p53 controlling oncogene-induced senescence, Aging (Albany NY) 2 (2010) 445–452.

[7] H. Bouamar, D. Jiang, L. Wang, A.P. Lin, M. Ortega, R.C. Aguiar, MicroRNA 155 control of p53 activity is context dependent and mediated by Aicda and Socs1, Mol. Cell. Biol. 35 (2015) 1329–1340.

[8] K. Shimada, S. Serada, M. Fujimoto, S. Nomura, R. Nakatsuka, E. Harada, et al., Molecular mechanism underlying the antiproliferative effect of suppressor of cytokine signaling-1 in non-small-cell lung cancer cells, Cancer Sci. 104 (2013) 1483–1491.

[9] O. Hatirnaz, U. Ure, C. Ar, C. Akyerli, T. Soysal, B. Ferhanoglu, et al., The SOCS-1 gene methylation in chronic myeloid leukemia patients, Am. J. Hematol. 82 (2007) 729–730.

[10] C.G. Ekmekci, M.I. Gutierrez, A.K. Siraj, U. Ozbek, K. Bhatia, Aberrant methylation of multiple tumor suppressor genes in acute myeloid leukemia, Am. J. Hematol. 77 (2004) 233–240.

[11] C.S. Chim, K.Y. Wong, F. Loong, G. Srivastava, SOCS1 and SHP1 hypermethylation in mantle cell lymphoma and follicular lymphoma: implications for epigenetic activation of the Jak/STAT pathway, Leukemia 18 (2004) 356–358.

[12] T.C. Liu, S.F. Lin, J.G. Chang, M.Y. Yang, S.Y. Hung, C.S. Chang, Epigenetic alteration of the SOCS1 gene in chronic myeloid leukaemia, Br. J. Haematol. 123 (2003) 654–661.

[13] L.F. Lu, T.H. Thai, D.P. Calado, A. Chaudhry, M. Kubo, K. Tanaka, et al., Foxp3-dependent microRNA155 confers competitive fitness to regulatory T cells by targeting SOCS1 protein, Immunity 30 (2009) 80–91.

[14] S. Jiang, H.W. Zhang, M.H. Lu, X.H. He, Y. Li, H. Gu, et al., MicroRNA-155 functions as an OncomiR in breast cancer by targeting the suppressor of cytokine signaling 1 gene, Cancer Res. 70 (2010) 3119–3127.

[15] O. Merkel, F. Hamacher, R. Griessl, L. Grabner, A.I. Schiefer, N. Prutsch, et al., Oncogenic role of miR-155 in anaplastic large cell lymphoma lacking the t(2;5) translocation, J. Pathol. 236 (2015) 445–456.

[16] F. Pichiorri, S.S. Suh, M. Ladetto, M. Kuehl, T. Palumbo, D. Drandi, et al., MicroRNAs regulate critical genes associated with multiple myeloma pathogenesis, Proc. Natl. Acad. Sci. U S A 105 (2008) 12885–12890.

[17] N. Kobayashi, H. Uemura, K. Nagahama, K. Okudela, M. Furuya, Y. Ino, et al., Identification of miR-30d as a novel prognostic maker of prostate cancer, Oncotarget 3 (2012) 1455–1471.

[18] F.A. Mallette, M.F. Gaumont-Leclerc, G. Huot, G. Ferbeyre, Myc down-regulation as a mechanism to activate the Rb pathway in STAT5A-induced senescence, J. Biol. Chem. 282 (2007) 34938–34944.

[19] J. Kluiver, J.H. Gibcus, C. Hettinga, A. Adema, M.K. Richter, N. Halsema, et al., Rapid generation of microRNA sponges for microRNA inhibition, PLoS ONE 7 (2012) e29275.

[20] T.R. Brummelkamp, R. Bernards, R. Agami, A system for stable expression of short interfering RNAs in mammalian cells, Science 296 (2002) 550–553.

[21] G. Ferbeyre, E. de Stanchina, E. Querido, N. Baptiste, C. Prives, S.W. Lowe, PML is induced by oncogenic ras and promotes premature senescence, Genes. Dev. 14 (2000) 2015–2027.

[22] F.A. Mallette, O. Moiseeva, V. Calabrese, B. Mao, M.F. Gaumont-Leclerc, G. Ferbeyre, Transcriptome analysis and tumor suppressor requirements of STAT5-induced senescence, Ann. N Y Acad. Sci. 1197 (2010) 142–151.

[23] X. Deschenes-Simard, M.F. Gaumont-Leclerc, V. Bourdeau, F. Lessard, O. Moiseeva, V. Forest, et al., Tumor suppressor activity of the ERK/MAPK pathway by promoting selective protein degradation, Genes. Dev. 27 (2013) 900–915.

[24] X.Z.J. Luo, H. Wang, Y. Du, L. Yang, F. Zheng, D. Ma, PolyA RT-PCR-based quantification of microRNA by using universal TaqMan probe, Biotechnol. Lett. 34 (2012) 627–633.

[25] M.A. Lokuta, M.A. McDowell, D.M. Paulnock, Identification of an additional isoform of STAT5 expressed in immature macrophages, J. Immunol. 161 (1998) 1594–1597.

[26] K.L. Kopp, U. Ralfkiaer, L.M. Gjerdrum, R. Helvad, I.H. Pedersen, T. Litman, et al., STAT5-mediated expression of oncogenic miR-155 in cutaneous T-cell lymphoma, Cell Cycle 12 (2013) 1939–1947 (Georgetown, Tex.).

[27] Y. Feuermann, G.W. Robinson, B.M. Zhu, K. Kang, N. Raviv, D. Yamaji, et al., The miR-17/92 cluster is targeted by STAT5 but dispensable for mammary development, Genesis 50 (2012) 665–671.

[28] J.E. Purvis, K.W. Karhohs, C. Mock, E. Batchelor, A. Loewer, G. Lahav, P53 dynamics control cell fate, Science 336 (2012) 1440–1444.

[29] I. Behm-Ansmant, J. Rehwinkel, T. Doerks, A. Stark, P. Bork, E. Izaurralde, MRNA degradation by miRNAs and GW182 requires both CCR4:NOT deadenylase and DCP1:DCP2 decapping complexes, Genes. Dev. 20 (2006) 1885–1898.

[30] G.K. Lambert, A.K. Duhme-Klair, T. Morgan, M.K. Ramjee, The background, discovery and clinical development of BCR-ABL inhibitors, Drug Discov. Today 18 (2013) 992–1000.

[31] A. Lujambio, S.W. Lowe, The microcosmos of cancer, Nature 482 (2012) 347–355.

[32] G. Marcucci, K. Mrozek, M.D. Radmacher, R. Garzon, C.D. Bloomfield, The prognostic and functional role of microRNAs in acute myeloid leukemia, Blood 117 (2011) 1121–1129.

[33] H.L. Janssen, H.W. Reesink, E.J. Lawitz, S. Zeuzem, M. Rodriguez-Torres, K. Patel, et al., Treatment of HCV infection by targeting microRNA, N Engl. J. Med. 368 (2013) 1685–1694.